Structural Engineering and Mechanics, *Vol. 74, No. 3 (2020) 381-394*
DOI: https://doi.org/10.12989/sem.2020.74.3.381

Behavior of CFS built-up battened columns: Parametric study and design recommendations

Vijayanand S[1a] and Anbarasu M*[2]

[1]*Department of Civil Engineering, Kongu Engineering College, Perundurai, Tamilnadu, India*
[2]*Department of Civil Engineering, Government College of Engineering, Salem, Tamilnadu, India*

(Received November 5, 2019, Revised December 3, 2019, Accepted December 12, 2019)

Abstract. The structural performance of cold-formed steel (CFS) built-up battened columns were numerically investigated in this paper. The built-up column sections were formed by connecting two-lipped channels back-to-back, with a regular spacing of battens plates, and have been investigated in the current study. Finite element models were validated with the test results reported by the authors in the companion paper. Using the validated models, the parametric study was extended, covering a wider range of overall slenderness to assess the accuracy of the current design rules in predicting the design strengths of the CFS built-up battened columns. The parameters viz., overall slenderness, different geometries, plate slenderness (b/t ratio) and yield stress were considered for this study. In total, a total of 228 finite element models were analyzed and the results obtained were compared with current design strength predicted by Effective Width Method of AISI Specifications (AISI S100:2016) and European specifications (EN1993-1-3:2006). The parametric study results indicated that the current design rules are limited in predicting the accuracy of the design strengths of CFS built-up battened columns. Therefore, a design equation was proposed for the AISI and EC3 specifications to predict the reliable design strength of the CFS Built-up battened columns and was also verified by the reliability analysis.

Keywords: cold-formed steel; effective width method; lipped channel; numerical study; battened column; reliability analysis; built-up columns

1. Introduction

Cold-formed steel (CFS) sections have gained popularity in research and their utility in the construction sector. CFS sections are commonly adopted since there are many advantages such as lightweight, high strength to weight ratio, high stiffness, easy of erection and construction, etc., The adoption of built-up sections in the recent years has increased as the single sections are weak in torsion (Whittle and Ramseyer, 2009). The built-up sections can be formed by connecting different elements.

Sahoo *et al.* (2007) used an improved design method with decreased spacing of battens in the expected plastic hinge region to satisfy the expected flexural strength when it is subjected to the combined axial load with increasing lateral loads. Young and Chen (2008) presented the test results of CFS built-up closed sections using intermedia te stiffeners to assess the reliability of direct strength method. Megnounif *et al.* (2008) proposed a design procedure to predict the axial strength of the CFS built-up columns based on direct strength method and effective width method. Shi *et al.* (2011) carried out the parametric study on high strength steel equal angle compression members by influencing plate slenderness and yield strength to study the effects of local buckling under axial compression. EI Aghoury *et al.* (2013a) investigated the behavior and strength of battened column members composed of slender angle sections. The study showed that the design strengths predicted by North American and European codes are generally conservative. Bandula *et al.* (2013) investigated the slender CFS compression members experimentally to provide adequate design guidelines both for hot-rolled and CFS column members. Anbarasu *et al.* (2013) studied the influence of stiffener ties in the behavior open section CFS Columns under axial compression with intermediate length. ValsaIpe *et al.* (2013) conducted experimental study on CFS structures to study its performance and economy. Kripka *et al.* (2013) validated the experimental results of CFS columns with the simulated annealing method. They concluded that the reduced cross-sectional area of columns yields excellent results. Anbarasu *et al.* (2014) investigated the CFS open section channel using spacers to control the failure due to distortional buckling and proposed the design equation using nonlinear regression analysis. Muftah *et al.* (2014) studied the effect of connection arrangement of built-up CFS sections under axial compression. They recommended providing the end distance of bolt as 20 mm to increase the column capacity. Dar *et al.* (2015a) carried out the research in developing CFS with different sectional profiles to avoid the premature buckling. El Aghoury *et al.* (2015b) extends the work for a group of battened beam-columns with variable angle legs and found that the Eurocode-3 is more reliable than the AISI 2007. Biggs *et al.* (2015) investigated the built-up compression members experimentally by varying the length, intermediate weld pattern, orientation, and thickness of the specimens to study the effect of geometrical properties of the built-up compression members. Dabaon *et al.* (2015)

*Corresponding author, Professor
E-mail: gceanbu@gmail.com

http://www.techno-press.com/journals/sem&subpage=7
ISSN: 1225-4568 (Print), 1598-6217 (Online)

investigated the CFS built-up battened columns experimentally. Zhang and Young (2015) concluded that the current direct strength method along with the modified direct strength method can be employed for the design of CFS built-up open section columns. Maia *et al.* (2016) performed a numerical and empirical study of double angle members joined by batten plates under concentric and eccentric axial compression. Lu *et al.* (2017) presented an equivalent simplified web local buckling model followed by the energy method for the cold-formed C-section column. Muthuraj *et al.* (2017) investigated the fixed ended CFS lipped channel numerically to study the effects of Local-Distortional interaction buckling mode. Zhou *et al.* (2017) investigated the CFS lipped channel sections experimentally and numerically and proposed new design rules to determine the accurate elastic distortional buckling critical stress under axial compression. The research on CFS built-up beams was also done by other researchers (Dar *et al.* 2015b, 2018a, 2019a, 2019b, Saleh *et al.* 2016, Serror *et al.* 2017). Zhang and Young (2018) investigated the CFS built-up closed section columns with web stiffeners by numerically. Ye *et al.* (2018) proposed a numerical model to examine the flexural strength and failure modes of CFS back-to-back channel beams review the efficiency of an optimization framework already proposed. Dar *et al.* (2019b) investigated the CFS laced built-up columns with unstiffened angle sections experimentally and numerically to study the effects of lacing configuration and lacing slenderness. Kherbouche and Megnounif (2019) validated test results with the developed nonlinear finite element model of thin-walled CFS built-up columns under uniform compression. Dar *et al.* (2018b, 2019b) validated the test results of CFS built-up laced columns sections with the developed finite element models using ABAQUS.

The plate elements of Cold-formed sections are normally thin with higher plate slenderness ratio and hence they buckle locally before yield stress is reached. The use of doubly symmetric section is to avoid the flexural/torsional buckling. Engineers and architects face problems in using CFS built-up member with battens in structures because of the lack of knowledge about the behaviour and the lack of design specifications for built-up cold formed steel compression members. However, it should be noted that there is no systematic study available for CFS built-up battened column axial compression behaviour. For CFS sections, currently available design guidelines such as EN1993-1-3:2006, AISI S100:2016 are based on the classification approach of cross section known as EWM, which does not take into account the interaction of the chords in the built-up battened columns. The effect of chord slenderness was also not considered in the previous studies. Therefore it is important to address these issues in the current design rules to assess the stability of built-up cold-formed steel members. This proposed research work has been done as an attempt to systematically study the behaviour and ultimate load carrying capacity of the built-up cold-formed steel column with battens.

This paper presents the design rules of CFS built-up columns by observing its behaviour and design by numerical analysis. The built-up column section is formed by joining two channels placed back to back and connected by batten plates with a gap of regular spacing. The finite element models were validated with test results of CFS built-up columns in terms of ultimate axial compressive load and obtained deformed characteristic curves. The parametric study was conducted by varying the parameters viz., overall slenderness, different geometries, plate slenderness (b/t ratio) and yield stress with the validated FEM. This extended study helped to apply the FEA results to verify the design strengths evaluated by AISI and European code specifications (EC3). Since the shortcomings were found in the prediction of the design strength of the built-up columns by both AISI and EC3, the modifications of the design rules were proposed to determine the accurate ultimate load-carrying capacity of the CFS built-up battened sections.

2. Summary of experimental investigation Vijayanand and Anbarasu 2019):

The research on built-up columns conducted experimentally by Vijayanand and Anbarasu (2019) is used to conduct the parametric study for the CFS built-up battened columns. The finite element model was validated with the test results available in the literature of Vijayanand and Anbarasu (2019). A detailed summary of tests conducted is described in this section. The built-up section consists of two channels placed back to back and connected by batten plates with spacing such that I_{xx} equals 1.5 times I_{yy} by using self-drilling screws by bolted connection whose screws is of 5 mm diameter The plate slenderness of the built-up columns is selected based on the geometric limitations of the North American Specification for the design (AISI S100-2016) of CFS structural members. To fix the length of the column, the slenderness ratio was varied from 20 to 50. The spacing between the channels has been kept at 55 mm. In two different sizes of the channels, width of flange and lip were kept as 50 mm and depth of web has been varied as 120 mm and 150 mm. The plate slenderness was kept as 1.2 mm and 1.6 mm. The material properties obtained from the conducted tensile tests on coupons were used. The columns' end support conditions have been made pinned with warping restrained by providing the spherical ball set up between the loading plate and platen. To record the accurate readings of LVDTs (Linear variable displacement transducers) and applied load, a data acquisition system was used. A loading hydraulic jack of 500 kN capacity with load cell of 100 tonnes capacity was used to test the specimens. The complete details of testing of the specimens will be found in the literature (Vijayanand and Anbarasu 2019).

3. Finite element modelling:

3.1 General

The sections of the CFS built-up battened columns were developed numerically by using the software ABAQUS/CAE 6.14-1. The developed finite element models of CFS built-up columns were validated with the test results in terms of

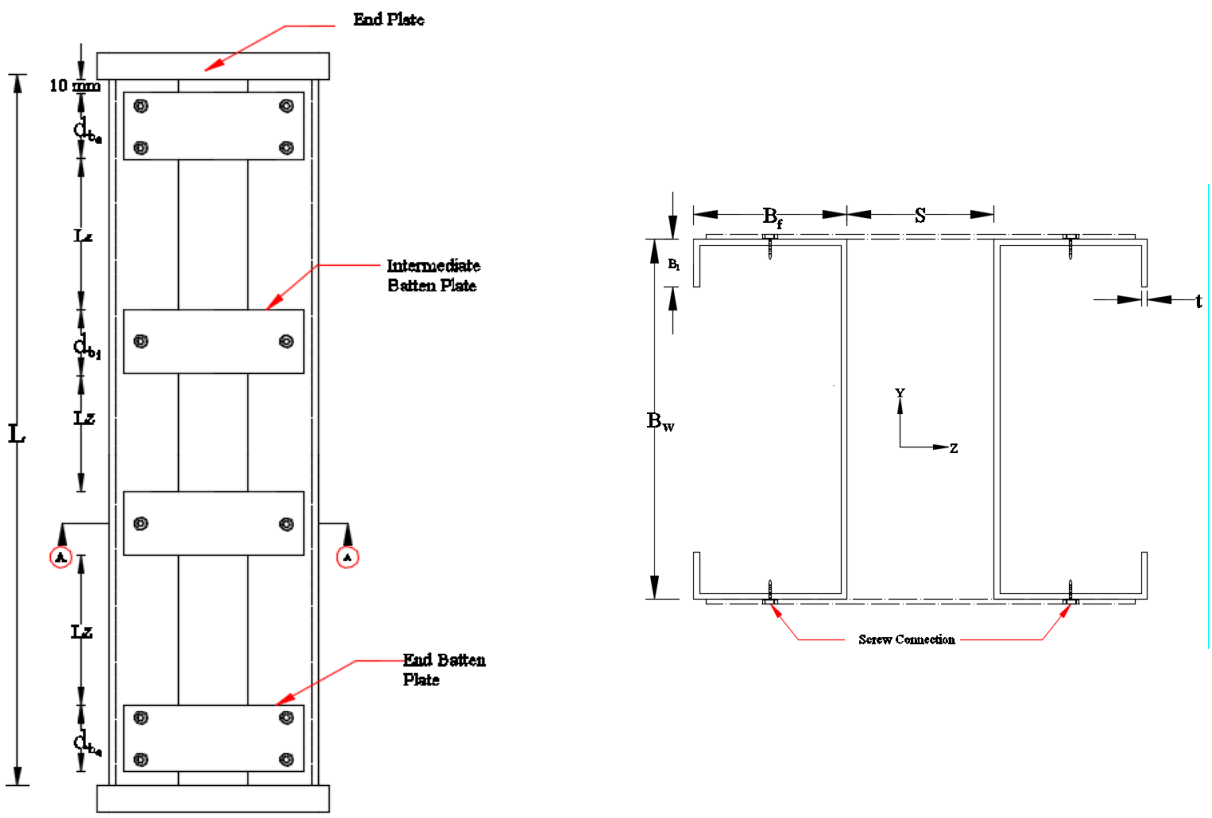

Fig. 1 Typical details of the specimen

ultimate axial compressive load and obtained deformed characteristic curves. The dimensions and material properties of the developed analytical models were based on the measured dimensions as presented in the literature. The typical geometrical details of the specimens were shown in Fig. 1.

3.2 Finite Element mesh

The modelling of the built-up columns and batten plates were done by fitting S4R (four-node doubly curved thin shell elements) with reduced integration and hourglass control permits finite membrane strains and rotations (Anbarasu *et al.* 2019b, Zhang and Young 2018, Saleh *et al.* 2016, Roy *et al.* 2018). The built-up sections were modelled with a mesh size of 5 mm x 5 mm in order to get an efficient finite element model.

3.3 Boundary conditions and loading method

The reference points were created at the centre of gravity of the built-up sections. Translational degree of freedom along 1, 2 and rotational degree of freedom along 3 were restricted at the loading edge of the built-up column and the degree of freedom of rotation along 3 was restrained and, at the other end, the degree of freedom of translation along 1, 2, 3 and the degree of freedom of rotation along 3 was restrained. The columns end support conditions have been made pin-ended by assigning translational constraints at the both ends using reference points created as detailed in the companion paper (Vijayanand and Anbarasu 2019).

The axial compressive load was applied through the created reference points of the upper end of the built-up columns. In constraint property, Tie (nodes) as region type with rigid body option available in the ABAQUS library was used in the finite element model to simulate the pin ended boundary conditions as followed by Anbarasu and Dar 2020.

3.4 Modelling of material, geometric imperfections, and connections

The material properties of the tensile coupons have been adopted in the FEM. The stress-strain curve measured was turned into a true stress-strain curve. The calculated true stress-strain values (ABAQUS manual 2014) were incorporated for the validation model to include the material non-linearity. In the parametric models, elastic perfectly plastic material models were included (Anbarasu *et al.* 2019a, Anbarasu *et al.* 2020). Initially a linear elastic buckling analysis of the built-up column was analyzed. In the step property, the number of Eigen vectors of 20 and the maximum number of iterations of 300 was specified with linear perturbation as buckle to obtain the mode shapes. Later, the obtained geometric imperfections from the mode shape were incorporated into the non-linear analysis. The local imperfection factor of 0.34t was used as the imperfection magnitude and global imperfection factor of L/1000 was applied in the nonlinear analysis for the parametric study (Schafer and Pecoz 1998). The global imperfection factor of L/1000 which was applied to the built-up column for the study. To make interaction between the channels and battens, the screw connections were defined based on ‘Point-based’ type of fasteners. (Ghanam

Table 1 Details of the specimens

Column Series	B_f (mm)	B_w (mm)	B_l (mm)	t (mm)	Spacing between the channels 'S' (mm)	Depth of End batten 'd_{be}'	Depth of Intermediate batten 'd_{bi}'
120x50x15-1.6	50	120	15	1.6	50	100	75
150x60x15-1.6	60	150	15	1.6	50	100	75
120x50x15-1.2	50	120	15	1.2	50	100	75
150x60x15-1.2	60	150	15	1.2	50	100	75

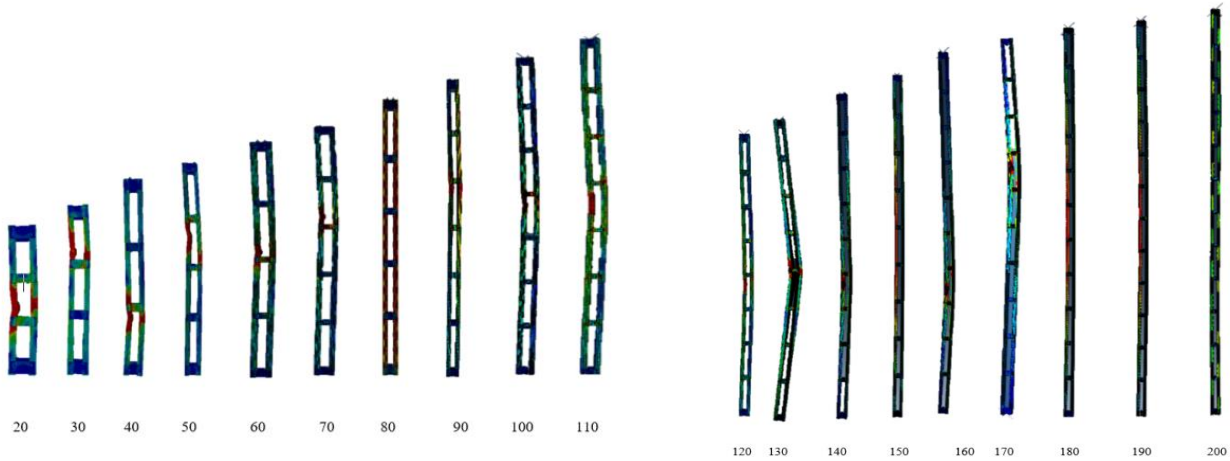

Fig. 3 Deformed shapes for 120x50x15-1.2 Series

et al. 2017). The attachment method used was 'face-to-face' and specified a search radius of 5 mm with physical radius of 10 mm.

4. Parametric study

The validated finite element model was used to carry out the parametric study for the investigation of the ultimate compressive resistance of the built-up columns. A total of 228 finite element models were analyzed. The factors which influence the parameters were overall slenderness, different geometries, Plate slenderness ratio, yield stress of the built-up columns. The overall slenderness ratio was varied from 20 to 200 in order to get accuracy in predicting the column strength. In this parametric study, the yield stress F_y was varied as 250, 350 and 450 MPa respectively. Every model has the same width of channel as 50 mm and spacing the channels were kept as 50 mm. The Plate slenderness of the models has been kept as 1.2 mm and 1.6 mm. The centre-to-centre spacing between the chords was calculated as per D1.2 of AISI S100-2016. Table 1 shows the cross-sectional dimensions of the CFS built-up battened columns. The models were labelled by depth of the channel section, width of the flange of channel, depth of lip followed by thickness and slenderness ratio with an example of 120x50x15-1.6-20-4. The load vs. axial shortening curve was displayed in Fig.2.

The deformed shapes of the built-up battened column for the series 120x50x15-1.2 were shown in Fig. 3. It is identified that the columns have undergone local buckling for the low global column slenderness (λ<60) and flexural buckling for high global slenderness (λ>130). The flexural

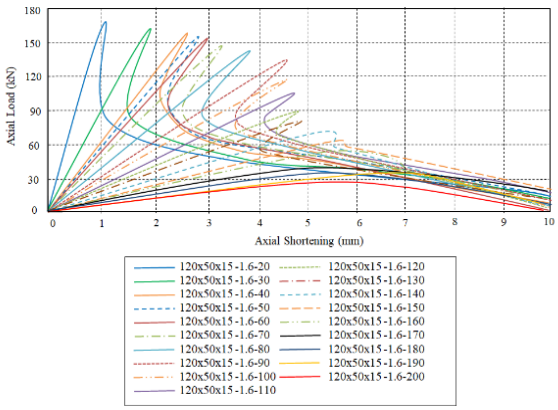

Fig. 2 Load vs. axial shortening curve for 120 x 50 x 15-1.2 Series

buckling occurs in the high global slenderness due to t he effect of plate slenderness. The columns have unde rgone interactive buckling (combination of local and fle xural buckling) for the global column slenderness (λ=6 0 to 130). Finally, the numerical analysis gets analyzed using ABAQUS and were compared with the design st rengths predicted by AISI (2016) and European specific ations (EC3) as shown in Table 2.

5. Design guidelines in accordance with the AISI-S100-2016 Standards

5.1 Effective width Method:

The numerical results of the finite element model (P_{FEA}) were compared with the un-factored design strengths predicted by the current design rules of the American Iron

and Steel Institute (AISI). As the axial compressive load predicted with specified guidelines of AISI is limited for CFS built-up battened columns, there is an attempt made to propose the equation for the built-up columns by using the Effective Width Method (EWM) in this study. The equations used by effective width method in accordance with AISI (2016) Specifications were mentioned below:

$$P_n = A_e F_n \quad (1)$$

Where, A_e = Effective area, mm^2, F_n = Critical buckling stress calculated The column strength results for P_{AISI} were shown in Table 2. The critical buckling stress (F_n) will be calculated as follows:

$$F_n = \left(0.658^{\lambda_c^2}\right) F_y, \quad \text{For } \lambda_c \leq 1.5 \quad (2)$$

$$F_n = \left(\frac{0.877}{\lambda_c^2}\right) F_y, \quad \text{For } \lambda_c > 1.5 \quad (3)$$

The non-dimensional critical slenderness (λc) will be calculated as follows:

$$\lambda_c = \sqrt{F_y / F_e} \quad (4)$$

Where F_y is the yield stress, and F_e is the least of elastic flexural, torsional, and flexural-torsional buckling stress.

According to clause I.1.2 of AISI-S100-2016, the modified slenderness was specified for the design of built-up compression members to account with impact of additional deformations made by longitudinal shear in the built-up sections. The evaluated modified slenderness ratio was used to calculate the results as per the given equation:

$$\left(\frac{kL}{r}\right)_m = \sqrt{\left(\frac{kL}{r}\right)_o + \left(\frac{a}{r_i}\right)_o} \quad (5)$$

where $(kL/r)_m$ is the modified slenderness ratio of built-up columns, $(KL/r)_o$ is the overall slenderness ratio of the entire cross-section of the built-up column, a = Screw spacing, r_i = minimum radius of gyration of the section. The effective width of plate elements has been determined as per the section B.2.1 of the AISI specifications.

5.2 European design rules (EC3):

The un-factored axial load (P_{EC3}) was calculated in accordance with EN 1993-1-3:2006 and EN 1993-1-1:2005 from the following given equation:

$$P_{EC3} = \chi A_g F_y / \gamma_{m1} \quad \text{(for Class 1, 2 or 3)} \quad (6)$$

$$= \chi A_e F_y / \gamma_{m1} \quad \text{(for Class 4)} \quad (7)$$

here A_e is the effective cross-sectional area for class 4 sections, A_g is gross cross-sectional area for class 1, 2 or 3 sections. 'χ' is the reduction factor, F_y is the yield stress which can be calculated as shown below:

$$\chi = \left(\frac{1}{\phi + \sqrt{\phi^2 - \bar{\lambda}^2}}\right) \quad \text{but} \quad \chi \leq 1.0 \quad (8)$$

$$\phi = 0.5\left[1 + \alpha\left(\bar{\lambda} - 0.2\right) + \bar{\lambda}^2\right] \quad (9)$$

The non-dimensional slenderness was calculated as given below:

$$\bar{\lambda} = \sqrt{\frac{A_g f_y}{N_{cr}}} \quad \text{(For Class 1, 2 or 3)} \quad (10)$$

$$\bar{\lambda} = \sqrt{\frac{A_e f_y}{N_{cr}}} \quad \text{(For Class 4)} \quad (11)$$

where'α' is the imperfection factor, 'N_{cr}' is the elastic critical buckling load for the relevant buckling mode based on the gross cross-sectional properties.

5.3 Reliability analysis

The reliability analysis was used in this study to assess the accuracy of the current design rule as an effective width method of AISI and EC3 of European specifications for the CFS built-up battened columns. The procedure for evaluating the reliability analysis was followed as per the commentary of the AISI Specifications. The target reliability index (β_0) was kept as lower limit of 2.5 for CFS built-up columns. In this study, the resistance factor (ϕ_c) was used as 0.85 for axially loaded compression members with load combinations of 1.2 DL+1.6 LL and 1.35 DL+1.5 LL in accordance with American Society of Civil Engineers (ASCE) standard and EC3 respectively where DL is the dead load and LL is the live load. From Table 2, it was observed that the reliability index (β) for both effective width method and EC3 method exceeds the target lower limit of 2.5.

6. Modified design guidelines

6.1 Proposed design equations in AISI

The calculated nominal design strengths were compared with the finite element models as shown in Fig. 4a and in Table 2. The current design curve predicts the safe results as an overall, but it is also shown that the results are more conservative particularly in the in-elastic region. Even though the reliability index value is higher than the target reliability index value, the results are not consistently scattered. Hence the modified design equation was proposed for the Effective width method of AISI (2016) as given in equations from (12)-(14).

The proposed curve was developed by fitting into the obtained data points as shown in Fig. 4a. A similar technique was also used for the curve proposal by other researchers such as Anbarasu and Dar (2020) and Gunalan and Mahendran (2013).

$$F_n = (0.720^{\lambda_c^{1.8}}) F_y, \quad \text{For } \lambda_c \leq 1.0 \quad (12)$$

$$F_n = (0.720^{\lambda_c^{2.1}}) F_y, \quad \text{For } 1.0 < \lambda_c \leq 1.5 \quad (13)$$

$$F_n = \left(\frac{1.10}{\lambda_c^{\,2}}\right) F_y, \qquad \text{For } \lambda_c \geq 1.5 \qquad (14)$$

The above-modified design equation is proposed in AISI-S100-2016. The same can also be applied in AS/NZ design guidelines also since they are similar to each other.

6.2 Proposed design equations in EC3:

Fig. 5a shows clearly that the non-linear finite element results presented were reliable and safe when compared with design buckling curves. But the results were scattered and unconservative particularly at the low non-dimensional slenderness of the built-up columns. Therefore, the design modification is proposed to determine the accurate load-carrying capacity of the CFS built-up battened columns as given in Eq. (15). The proposed curve which is a multi-stage curve was developed by fitting into the obtained data points as shown in Fig. 5a. A similar technique was also used for the curve proposal by other researchers such as Anbarasu and Dar (2020) and Devi and Singh (2020).

$$\chi = \begin{cases} 1.0 & for\ \bar{\lambda} \leq 0.2 \\ 1.025 + (0.15 - 0.99\,\bar{\lambda}) & for\ 0.2 < \bar{\lambda} \leq 0.3 \\ \left(\frac{0.646}{\bar{\lambda}^{\,0.25842}}\right) & for\ 0.3 < \bar{\lambda} \leq 1.0 \\ \left(\frac{3.535}{\bar{\lambda}^{\,1.842}}\right) - \left(\frac{2.872}{\bar{\lambda}^{\,2.089}}\right) & for\ 1.0 < \bar{\lambda} \leq 1.3 \\ \left(\frac{1.097}{\bar{\lambda}^{\,2.419}}\right) & for\ 1.3 < \bar{\lambda} \leq 1.6 \\ \left(\frac{1.0525}{\bar{\lambda}^{\,2.196}}\right) & for\ 1.6 < \bar{\lambda} \end{cases} \qquad (15)$$

7. Comparison of numerical strengths against the current design guidelines

7.1 General discussions:

The Figs. 4a and 5a show the comparison of parametric FEA results with current design curves of AISI and EC3 respectively and the test results available in the literature (Vijayanand and Anbarasu 2019). The proposed FEA points of AISI and EC3 are compared with the parametric FEA results in Figs. 4b and 5b respectively. The un-factored design strengths predicted by effective width method (P_{EWM}) of the current design rule of AISI and EC3 (P_{EC3}) were compared with the finite element models (P_{FEA}) as presented in Table 2. The value of mean and standard deviation of P_{FEM}/P_{AISI} is 1.38 and 0.267 respectively. The coefficient of variance and reliability index, β value of P_{FEM}/P_{AISI} is 0.193 and 3.28 respectively. As shown in Fig. 4a, the existing design curve shows the safer results at elastic and plastic regions and but particularly more conservative at the in-elastic region of the design curve. For moderate slenderness ratio (λ_c> 1.0 and λ_c< 2.0), the finite element results give more conservative results. Therefore, there is a scope for improvement in the existing design curve of AISI for the accurate design strength prediction for the built-up battened columns.

As shown in Fig. 4b, the obtained proposed AISI is reliable and safe since the mean value of proposed $P_{FEM}/P\#_{AISI}$ is 1.16 which is lesser than the mean value of the current AISI. The standard deviation and coefficient of variance are 0.175 and 0.150. Also, the reliability index, β

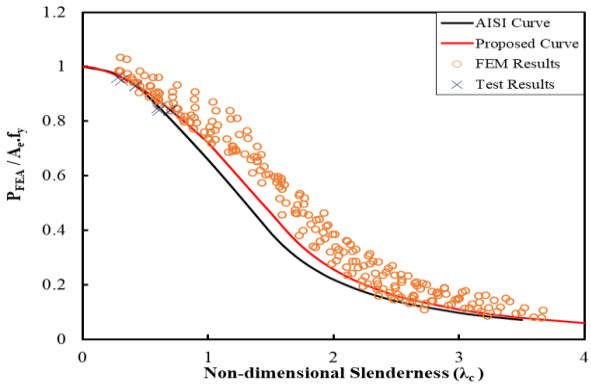

(a)

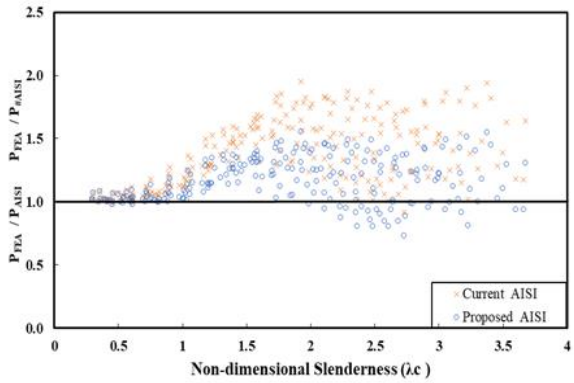

(b)

Fig. 4 Comparison of FEA results with AISI (2016) and Proposed AISI (2016)

for the proposed AISI is 2.97 which has crossed the target reliability value (β_0) of 2.5. Hence it is proved that the proposed design rules give safe and consistent results than the existing design if we see in Fig. 4b.

In EC3 approach, the calculated value of the mean and standard deviation of P_{FEM}/P_{EC3} is 1.42 and 0.320 respectively. The coefficient of variance and reliability index, β value of P_{FEM}/P_{EC3} is 0.226 and 3.04 respectively. The EC3 specifications give reliable results for the prediction of CFS built-up column and the reliability index value of EC3 exceeds the target reliability index (β_0) of 2.5. From Fig. 5a, it is shown that the finite element results are safe and the 'b' curve of EC3 predicts the better prediction of design strength of built-up columns.

But the finite element results are more conservative at the low non-dimensional slenderness value when compared with the current design curves of EC3. Therefore, the design modification is proposed for EC3 to determine the accurate load-carrying capacity of the CFS built-up battened columns. As shown in Fig. 5b, the obtained proposed EC3 gives consistent and safe results since the mean value of proposed $P_{FEM}/P\#_{EC3}$ is 1.25 which is lesser than the mean value of the current EC3. Also, the reliability index, β for the proposed EC3 is 2.87 which has crossed the target reliability value (β_0) of 2.50. If we see in Fig. 5b, it is proved that the proposed design rule of EC3 gives safe and consistent results than the existing design.

Table 2 Comparison of numerical strength with design strengths

Specimen ID	P_{FEA} (kN)	Design strength predicted by the current design rules						Design strength predicted by the proposed equations	
		AISI			EC3				
		λ_c	F_n (MPa)	P_{FEA}/P_{AISI}	$\bar{\lambda}$	χ	P_{FEA}/P_{EC3}	$P_{FEA}/P\#_{AISI}$	$P_{FEA}/P\#_{EC3}$
120x50x15 -1.6-20-4	165.23	0.305	240.48	1.07	0.275	0.962	1.09	1.07	1.16
120x50x15 -1.6-30-4	158.54	0.456	229.19	1.07	0.411	0.891	1.13	1.06	1.24
120x50x15 -1.6-40-4	156.28	0.605	214.47	1.12	0.546	0.817	1.21	1.10	1.31
120x50x15 -1.6-50-5	153.85	0.753	197.22	1.18	0.680	0.737	1.32	1.14	1.37
120x50x15 -1.6-60-5	151.76	0.898	178.39	1.27	0.811	0.655	1.47	1.19	1.41
120x50x15 -1.6-70-6	148.00	1.040	158.93	1.37	0.939	0.576	1.63	1.24	1.43
120x50x15 -1.6-80-6	145.35	1.180	139.64	1.50	1.065	0.503	1.83	1.33	1.46
120x50x15 -1.6-90-7	135.42	1.315	121.17	1.57	1.188	0.440	1.95	1.37	1.51
120x50x15 -1.6-100-7	115.00	1.448	104.00	1.52	1.307	0.386	1.89	1.29	1.27
120x50x15 -1.6-110-8	104.00	1.576	88.30	1.58	1.423	0.341	1.93	1.31	1.41
120x50x15 -1.6-120-9	89.87	1.700	75.87	1.56	1.535	0.304	1.88	1.24	1.46
120x50x15 -1.6-130-10	81.36	1.820	66.21	1.59	1.643	0.272	1.89	1.27	1.56
120x50x15 -1.6-140-11	71.11	1.935	58.54	1.57	1.747	0.246	1.83	1.25	1.46
120x50x15 -1.6-150-12	63.50	2.047	52.35	1.56	1.848	0.224	1.79	1.25	1.47
120x50x15 -1.6-160-13	55.32	2.153	47.28	1.51	1.944	0.206	1.70	1.20	1.43
120x50x15 -1.6-170-14	44.50	2.256	43.09	1.33	2.037	0.190	1.48	1.06	1.28
120x50x15 -1.6-180-15	39.00	2.354	39.57	1.27	2.125	0.177	1.40	1.01	1.23
120x50x15 -1.6-190-16	33.00	2.448	36.59	1.16	2.210	0.165	1.27	0.93	1.13
120x50x15 -1.6-200-17	29.98	2.538	34.05	1.14	2.320	0.151	1.26	0.91	1.15
150x60x15 -1.6-20-4	159.56	0.301	240.72	1.02	0.254	0.973	0.91	1.02	0.97
150x60x15 -1.6-30-5	148.04	0.450	229.66	0.98	0.380	0.908	0.91	0.98	1.00
150x60x15 -1.6-40-5	150.17	0.599	215.14	1.05	0.506	0.840	1.00	1.03	1.09
150x60x15 -1.6-50-5	141.97	0.747	197.98	1.07	0.630	0.767	1.03	1.03	1.09
150x60x15 -1.6-60-5	138.80	0.893	179.08	1.14	0.754	0.691	1.12	1.06	1.11
150x60x15 -1.6-70-6	139.01	1.037	159.34	1.25	0.876	0.615	1.26	1.14	1.16
150x60x15 -1.6-80-6	143.87	1.180	139.59	1.45	0.996	0.542	1.48	1.29	1.24
150x60x15 -1.6-90-7	134.54	1.321	120.49	1.53	1.115	0.476	1.57	1.33	1.24
150x60x15 -1.6-100-8	113.01	1.459	102.59	1.47	1.232	0.419	1.50	1.24	1.15
150x60x15 -1.6-110-8	87.89	1.595	86.24	1.32	1.346	0.370	1.32	1.09	0.92
150x60x15 -1.6-120-9	75.46	1.728	73.46	1.29	1.458	0.328	1.28	1.03	0.96
150x60x15 -1.6-130-9	68.37	1.858	63.52	1.32	1.568	0.293	1.30	1.05	1.03
150x60x15 -1.6-140-10	57.27	1.985	55.63	1.13	1.676	0.264	1.21	0.90	0.94
150x60x15 -1.6-150-11	49.54	2.109	49.27	1.05	1.780	0.239	1.16	0.84	0.93
150x60x15 -1.6-160-11	45.82	2.231	44.06	1.05	1.882	0.218	1.17	0.84	0.97
150x60x15 -1.6-170-12	39.86	2.349	39.75	1.06	1.982	0.199	1.12	0.84	0.95
150x60x15 -1.6-180-12	33.90	2.463	36.13	1.06	2.078	0.184	1.03	0.84	0.90
150x60x15 -1.6-190-13	30.54	2.575	33.07	1.06	2.172	0.170	1.00	0.85	0.89
150x60x15 -1.6-200-14	28.14	2.683	30.45	1.06	2.879	0.103	1.53	0.85	1.52
120x50x15 -1.2-20-4	103.353	0.420	232.24	1.01	0.260	0.969	0.99	1.01	1.06
120x50x15 -1.2-30-4	102.151	0.458	228.96	1.01	0.390	0.903	1.06	1.00	1.16
120x50x15 -1.2-40-4	99.134	0.610	213.97	1.03	0.519	0.832	1.11	1.01	1.21
120x50x15 -1.2-50-5	96.698	0.760	196.30	1.08	0.647	0.757	1.19	1.03	1.25
120x50x15 -1.2-60-5	92.273	0.909	176.90	1.12	0.774	0.679	1.27	1.05	1.25
120x50x15 -1.2-70-6	90.458	1.056	156.71	1.22	0.899	0.600	1.40	1.11	1.27

120x50x15 -1.2-80-6	85.314	1.202	136.58	1.29	1.023	0.527	1.51	1.15	1.22
120x50x15 -1.2-90-7	81.243	1.345	117.23	1.40	1.145	0.461	1.64	1.21	1.28
120x50x15 -1.2-100-7	76.622	1.486	99.19	1.53	1.265	0.404	1.77	1.29	1.15
120x50x15 -1.2-110-8	65.00	1.625	83.06	1.50	1.383	0.356	1.70	1.20	1.21
120x50x15 -1.2-120-9	53.00	1.761	70.73	1.41	1.498	0.315	1.57	1.12	1.20
120x50x15 -1.2-130-10	48.75	1.894	61.13	1.46	1.612	0.281	1.62	1.17	1.23
120x50x15 -1.2-140-11	40.00	2.024	53.52	1.35	1.723	0.252	1.48	1.07	1.17
120x50x15 -1.2-150-12	34.15	2.151	47.38	1.28	1.831	0.228	1.40	1.02	1.14
120x50x15 -1.2-160-13	28.97	2.275	42.35	1.19	1.937	0.207	1.30	0.95	1.10
120x50x15 -1.2-170-14	26.80	2.396	38.19	1.21	2.040	0.190	1.32	0.96	1.14
120x50x15 -1.2-180-15	23.98	2.514	34.69	1.18	2.140	0.175	1.28	0.94	1.13
120x50x15 -1.2-190-16	21.90	2.628	31.74	1.18	2.237	0.161	1.26	0.94	1.14
120x50x15 -1.2-200-17	19.10	2.739	29.22	1.12	2.332	0.150	1.19	0.89	1.09
150x60x15 -1.2-20-4	107.965	0.292	241.25	1.02	0.241	0.979	0.91	1.02	0.96
150x60x15 -1.2-30-5	104.543	0.437	230.78	1.02	0.361	0.918	0.94	1.01	1.03
150x60x15 -1.2-40-5	102.066	0.582	216.93	1.04	0.481	0.854	0.99	1.02	1.08
150x60x15 -1.2-50-5	99.719	0.727	200.44	1.08	0.600	0.785	1.05	1.04	1.12
150x60x15 -1.2-60-5	96.167	0.870	182.10	1.13	0.719	0.713	1.11	1.06	1.13
150x60x15 -1.2-70-6	92.548	1.013	162.74	1.19	0.836	0.639	1.19	1.09	1.13
150x60x15 -1.2-80-6	89.158	1.154	143.12	1.28	0.953	0.568	1.30	1.14	1.12
150x60x15 -1.2-90-7	84.465	1.295	123.94	1.37	1.069	0.501	1.39	1.19	1.11
150x60x15 -1.2-100-8	73.165	1.434	105.74	1.35	1.184	0.442	1.37	1.15	1.06
150x60x15 -1.2-110-8	67.862	1.571	88.79	1.45	1.297	0.390	1.44	1.21	1.07
150x60x15 -1.2-120-9	62.135	1.707	75.21	1.53	1.410	0.346	1.48	1.22	1.07
150x60x15 -1.2-130-5	47.12	1.842	64.64	1.31	1.521	0.308	1.26	1.05	0.98
150x60x15 -1.2-140-6	45.452	1.974	56.26	1.42	1.630	0.276	1.36	1.13	1.04
150x60x15 -1.2-150-6	38.587	2.105	49.49	1.34	1.738	0.249	1.28	1.07	1.02
150x60x15 -1.2-160-7	28.56	2.233	43.95	1.10	1.844	0.225	1.05	0.87	0.86
150x60x15 -1.2-170-8	24.077	2.360	39.36	1.01	1.948	0.205	0.97	0.81	0.82
150x60x15 -1.2-180-8	22.07	2.485	35.52	1.01	2.051	0.188	0.97	0.81	0.84
150x60x15 -1.2-190-9	20.339	2.607	32.26	1.01	2.152	0.173	0.97	0.81	0.86
150x60x15 -1.2-200-9	17.14	2.727	29.48	0.92	2.251	0.160	0.89	0.73	0.80
120x50x15 -1.6-20-4	207.24	0.360	331.48	1.03	0.317	0.940	1.05	1.03	1.13
120x50x15 -1.6-30-4	200.55	0.539	309.91	1.05	0.475	0.857	1.11	1.03	1.22
120x50x15 -1.6-40-4	198.29	0.716	282.40	1.12	0.631	0.767	1.23	1.08	1.30
120x50x15 -1.6-50-5	195.86	0.891	251.11	1.23	0.785	0.672	1.39	1.15	1.35
120x50x15 -1.6-60-5	190.21	1.062	218.21	1.34	0.936	0.578	1.56	1.21	1.38
120x50x15 -1.6-70-6	188.65	1.231	185.62	1.53	1.084	0.493	1.82	1.35	1.45
120x50x15 -1.6-80-6	169.05	1.396	154.86	1.60	1.229	0.420	1.91	1.37	1.46
120x50x15 -1.6-90-7	145.00	1.556	126.70	1.62	1.371	0.360	1.91	1.35	1.35
120x50x15 -1.6-100-7	125.00	1.713	104.63	1.65	1.509	0.312	1.91	1.31	1.47
120x50x15 -1.6-110-8	114.00	1.865	88.30	1.74	1.642	0.273	1.99	1.38	1.53
120x50x15 -1.6-120-9	102.00	2.011	75.87	1.77	1.772	0.241	2.01	1.41	1.62
120x50x15 -1.6-130-10	87.00	2.153	66.21	1.70	1.897	0.215	1.93	1.36	1.60
120x50x15 -1.6-140-11	75.00	2.290	58.54	1.65	2.017	0.193	1.84	1.32	1.58
120x50x15 -1.6-150-12	67.00	2.422	52.35	1.65	2.133	0.175	1.82	1.32	1.60
120x50x15 -1.6-160-13	59.00	2.548	47.28	1.61	2.244	0.161	1.75	1.28	1.57
120x50x15 -1.6-170-14	53.00	2.669	43.09	1.59	2.351	0.148	1.70	1.27	1.57

120x50x15 -1.6-180-15	47.60	2.785	39.57	1.55	2.453	0.137	1.65	1.24	1.54
120x50x15 -1.6-190-16	45.12	2.896	36.59	1.59	2.551	0.128	1.68	1.27	1.59
120x50x15 -1.6-200-17	40.36	3.002	34.05	1.53	2.678	0.117	1.64	1.22	1.59
150x60x15 -1.6-20-4	221.00	0.356	331.94	1.08	0.293	0.953	0.97	1.08	1.05
150x60x15 -1.6-30-5	194.36	0.533	310.80	1.00	0.439	0.876	0.93	0.99	1.02
150x60x15 -1.6-40-5	185.88	0.709	283.63	1.03	0.585	0.795	0.98	1.00	1.05
150x60x15 -1.6-50-5	174.25	0.883	252.47	1.07	0.729	0.707	1.03	1.00	1.04
150x60x15 -1.6-60-5	169.00	1.056	219.39	1.17	0.871	0.618	1.14	1.06	1.05
150x60x15 -1.6-70-6	164.00	1.227	186.30	1.30	1.012	0.533	1.28	1.15	1.04
150x60x15 -1.6-80-6	159.74	1.396	154.78	1.47	1.151	0.458	1.46	1.26	1.14
150x60x15 -1.6-90-7	151.00	1.562	125.73	1.66	1.288	0.394	1.60	1.38	1.20
150x60x15 -1.6-100-8	138.50	1.726	103.03	1.79	1.423	0.341	1.70	1.43	1.24
150x60x15 -1.6-110-8	119.24	1.887	86.24	1.79	1.555	0.297	1.68	1.42	1.32
150x60x15 -1.6-120-9	85.14	2.044	73.46	1.46	1.685	0.261	1.36	1.16	1.06
150x60x15 -1.6-130-9	74.52	2.198	63.52	1.44	1.812	0.232	1.34	1.15	1.09
150x60x15 -1.6-140-10	62.56	2.349	55.63	1.35	1.936	0.207	1.26	1.08	1.06
150x60x15 -1.6-150-11	55.73	2.496	49.27	1.33	2.057	0.187	1.25	1.06	1.08
150x60x15 -1.6-160-11	48.37	2.639	44.06	1.27	2.175	0.170	1.19	1.02	1.06
150x60x15 -1.6-170-12	42.91	2.779	39.75	1.24	2.290	0.155	1.16	0.99	1.05
150x60x15 -1.6-180-12	37.65	2.915	36.13	1.26	2.402	0.142	1.10	1.00	1.02
150x60x15 -1.6-190-13	33.99	3.047	33.07	1.18	2.510	0.131	1.08	0.94	1.02
150x60x15 -1.6-200-14	30.50	3.175	30.45	1.15	3.326	0.079	1.62	0.92	1.69
120x50x15 -1.2-20-4	134.25	0.496	315.69	1.07	0.293	0.953	1.04	1.06	1.12
120x50x15 -1.2-30-4	129.85	0.542	309.46	1.05	0.439	0.877	1.09	1.04	1.20
120x50x15 -1.2-40-4	128.54	0.722	281.47	1.10	0.584	0.795	1.19	1.07	1.28
120x50x15 -1.2-50-5	127.60	0.899	249.48	1.19	0.728	0.707	1.33	1.11	1.34
120x50x15 -1.2-60-5	123.17	1.076	215.66	1.27	0.870	0.618	1.47	1.15	1.35
120x50x15 -1.2-70-6	121.36	1.250	182.01	1.44	1.011	0.533	1.68	1.27	1.36
120x50x15 -1.2-80-6	112.70	1.422	150.15	1.58	1.151	0.458	1.81	1.35	1.41
120x50x15 -1.2-90-7	94.65	1.592	121.17	1.59	1.288	0.394	1.77	1.32	1.33
120x50x15 -1.2-100-7	82.00	1.758	99.27	1.63	1.423	0.341	1.77	1.30	1.29
120x50x15 -1.2-110-8	71.02	1.922	83.06	1.64	1.556	0.297	1.76	1.31	1.39
120x50x15 -1.2-120-9	59.717	2.083	70.73	1.58	1.686	0.261	1.68	1.26	1.32
120x50x15 -1.2-130-10	51.21	2.241	61.13	1.54	1.813	0.232	1.63	1.23	1.32
120x50x15 -1.2-140-11	45.53	2.395	53.52	1.53	1.938	0.207	1.62	1.22	1.36
120x50x15 -1.2-150-12	41.32	2.545	47.38	1.54	2.060	0.186	1.63	1.23	1.41
120x50x15 -1.2-160-13	37.00	2.692	42.35	1.52	2.179	0.169	1.61	1.21	1.43
120x50x15 -1.2-170-14	32.50	2.835	38.19	1.46	2.295	0.154	1.55	1.17	1.41
120x50x15 -1.2-180-15	29.75	2.974	34.69	1.46	2.407	0.142	1.55	1.17	1.43
120x50x15 -1.2-190-16	26.14	3.110	31.74	1.41	2.517	0.131	1.47	1.12	1.39
120x50x15 -1.2-200-17	23.65	3.241	29.22	1.38	2.623	0.121	1.43	1.10	1.38
150x60x15 -1.2-20-4	130.57	0.345	332.97	1.00	0.272	0.963	0.88	1.00	0.94
150x60x15 -1.2-30-5	127.15	0.517	312.91	1.01	0.408	0.893	0.92	1.00	1.01
150x60x15 -1.2-40-5	124.67	0.689	286.95	1.05	0.543	0.818	0.98	1.02	1.06
150x60x15 -1.2-50-5	119.53	0.860	256.88	1.08	0.678	0.738	1.05	1.02	1.08
150x60x15 -1.2-60-5	112.35	1.030	224.59	1.12	0.812	0.654	1.11	1.02	1.06
150x60x15 -1.2-70-6	115.15	1.198	191.88	1.29	0.945	0.572	1.30	1.14	1.13
150x60x15 -1.2-80-6	111.76	1.366	160.30	1.46	1.078	0.496	1.45	1.26	1.16
150x60x15 -1.2-90-7	103.00	1.532	130.79	1.60	1.209	0.430	1.55	1.33	1.19

150x60x15 -1.2-100-8	82.34	1.696	106.65	1.51	1.338	0.373	1.42	1.21	0.98
150x60x15 -1.2-110-8	74.00	1.859	88.79	1.58	1.467	0.326	1.47	1.26	1.10
150x60x15 -1.2-120-9	64.15	2.020	75.21	1.58	1.594	0.286	1.45	1.26	1.17
150x60x15 -1.2-130-5	55.47	2.179	64.64	1.55	1.719	0.253	1.41	1.23	1.12
150x60x15 -1.2-140-6	47.87	2.336	56.26	1.50	1.843	0.226	1.37	1.19	1.12
150x60x15 -1.2-150-6	39.94	2.490	49.49	1.39	1.964	0.202	1.27	1.11	1.08
150x60x15 -1.2-160-7	32.654	2.643	43.95	1.25	2.085	0.183	1.15	1.00	1.01
150x60x15 -1.2-170-8	29.47	2.792	39.36	1.24	2.203	0.166	1.15	0.99	1.02
150x60x15 -1.2-180-8	27.48	2.940	35.52	1.26	2.319	0.152	1.17	1.00	1.07
150x60x15 -1.2-190-9	25.14	3.085	32.26	1.25	2.433	0.139	1.17	1.00	1.09
150x60x15 -1.2-200-9	19.01	3.227	29.48	1.02	2.545	0.128	0.96	0.81	0.91
120x50x15 -1.6-20-4	236.53	0.409	419.62	1.01	0.349	0.924	1.01	1.00	1.10
120x50x15 -1.6-30-4	221.84	0.611	384.85	1.00	0.522	0.830	1.05	0.98	1.14
120x50x15 -1.6-40-4	215.49	0.812	341.50	1.05	0.694	0.729	1.16	1.00	1.19
120x50x15 -1.6-50-5	204.82	1.010	293.64	1.12	0.863	0.623	1.29	1.02	1.20
120x50x15 -1.6-60-5	200.14	1.205	245.13	1.28	1.029	0.523	1.50	1.13	1.21
120x50x15 -1.6-70-6	197.69	1.396	199.11	1.51	1.192	0.437	1.78	1.29	1.37
120x50x15 -1.6-80-6	181.16	1.583	157.56	1.68	1.352	0.368	1.94	1.40	1.35
120x50x15 -1.6-90-7	157.30	1.765	126.70	1.76	1.508	0.312	1.98	1.40	1.52
120x50x15 -1.6-100-7	135.25	1.942	104.63	1.78	1.659	0.268	1.98	1.42	1.54
120x50x15 -1.6-110-8	120.19	2.114	88.30	1.83	1.806	0.233	2.03	1.46	1.64
120x50x15 -1.6-120-9	104.71	2.281	75.87	1.82	1.948	0.205	2.01	1.45	1.69
120x50x15 -1.6-130-10	90.00	2.441	66.21	1.76	2.086	0.182	1.94	1.40	1.69
120x50x15 -1.6-140-11	81.00	2.597	58.54	1.79	2.218	0.164	1.94	1.42	1.74
120x50x15 -1.6-150-12	70.00	2.746	52.35	1.73	2.346	0.148	1.85	1.38	1.70
120x50x15 -1.6-160-13	65.00	2.889	47.28	1.77	2.468	0.136	1.89	1.41	1.77
120x50x15 -1.6-170-14	60.00	3.027	43.09	1.80	2.585	0.125	1.89	1.43	1.81
120x50x15 -1.6-180-15	55.00	3.158	39.57	1.79	2.698	0.115	1.87	1.43	1.82
120x50x15 -1.6-190-16	50.00	3.284	36.59	1.76	2.805	0.108	1.83	1.41	1.80
120x50x15 -1.6-200-17	48.00	3.404	34.05	1.82	2.945	0.098	1.92	1.45	1.92
150x60x15 -1.6-20-4	241.12	0.403	420.37	1.02	0.324	0.937	0.88	1.01	0.96
150x60x15 -1.6-30-5	228.67	0.604	386.26	1.02	0.484	0.852	0.92	1.00	1.01
150x60x15 -1.6-40-5	219.10	0.804	343.41	1.05	0.645	0.759	0.99	1.00	1.04
150x60x15 -1.6-50-5	208.64	1.000	295.69	1.12	0.803	0.660	1.09	1.02	1.05
150x60x15 -1.6-60-5	200.15	1.198	246.84	1.25	0.961	0.563	1.22	1.11	1.05
150x60x15 -1.6-70-6	196.57	1.392	200.04	1.47	1.116	0.476	1.42	1.26	1.12
150x60x15 -1.6-80-6	181.47	1.583	157.46	1.65	1.269	0.402	1.55	1.37	1.17
150x60x15 -1.6-90-7	168.90	1.772	125.73	1.85	1.421	0.342	1.70	1.48	1.24
150x60x15 -1.6-100-8	141.00	1.957	103.03	1.82	1.569	0.293	1.65	1.45	1.31
150x60x15 -1.6-110-8	121.00	2.139	86.24	1.81	1.715	0.254	1.64	1.45	1.29
150x60x15 -1.6-120-9	101.65	2.318	73.46	1.74	1.858	0.222	1.57	1.39	1.29
150x60x15 -1.6-130-9	85.70	2.493	63.52	1.66	1.998	0.197	1.50	1.32	1.28
150x60x15 -1.6-140-10	78.25	2.663	55.63	1.69	2.135	0.175	1.53	1.35	1.35
150x60x15 -1.6-150-11	65.32	2.830	49.27	1.56	2.268	0.158	1.42	1.25	1.29
150x60x15 -1.6-160-11	56.47	2.993	44.06	1.49	2.398	0.143	1.36	1.19	1.26
150x60x15 -1.6-170-12	44.18	3.151	39.75	1.28	2.525	0.130	1.17	1.02	1.10
150x60x15 -1.6-180-12	39.66	3.305	36.13	1.23	2.648	0.119	1.14	0.98	1.10
150x60x15 -1.6-190-13	37.00	3.455	33.07	1.28	2.768	0.110	1.15	1.02	1.13

150x60x15 -1.6-200-14	31.25	3.600	30.45	1.18	3.668	0.065	1.64	0.94	1.77
120x50x15 -1.2-20-4	157.26	0.563	394.10	1.09	0.317	0.940	1.05	1.08	1.14
120x50x15 -1.2-30-4	149.43	0.615	384.13	1.06	0.475	0.857	1.09	1.03	1.20
120x50x15 -1.2-40-4	141.74	0.818	340.05	1.08	0.632	0.766	1.16	1.03	1.22
120x50x15 -1.2-50-5	139.59	1.020	291.18	1.17	0.788	0.669	1.31	1.07	1.28
120x50x15 -1.2-60-5	135.63	1.220	241.45	1.29	0.943	0.574	1.48	1.14	1.30
120x50x15 -1.2-70-6	127.87	1.417	194.13	1.44	1.096	0.487	1.65	1.23	1.31
120x50x15 -1.2-80-6	121.00	1.612	151.80	1.68	1.246	0.412	1.84	1.34	1.40
120x50x15 -1.2-90-7	100.47	1.805	121.17	1.69	1.395	0.351	1.80	1.35	1.29
120x50x15 -1.2-100-7	87.52	1.994	99.27	1.74	1.541	0.301	1.82	1.39	1.43
120x50x15 -1.2-110-8	77.00	2.180	83.06	1.78	1.685	0.261	1.85	1.42	1.44
120x50x15 -1.2-120-9	68.00	2.362	70.73	1.80	1.826	0.229	1.86	1.44	1.52
120x50x15 -1.2-130-10	58.00	2.541	61.13	1.74	1.964	0.202	1.80	1.39	1.52
120x50x15 -1.2-140-11	51.00	2.715	53.52	1.72	2.099	0.180	1.77	1.37	1.55
120x50x15 -1.2-150-12	48.00	2.886	47.38	1.79	2.231	0.162	1.86	1.43	1.67
120x50x15 -1.2-160-13	45.36	3.053	42.35	1.87	2.360	0.147	1.94	1.49	1.78
120x50x15 -1.2-170-14	42.19	3.215	38.19	1.90	2.485	0.134	1.98	1.52	1.86
120x50x15 -1.2-180-15	39.46	3.373	34.69	1.94	2.608	0.123	2.02	1.55	1.93
120x50x15 -1.2-190-16	30.26	3.526	31.74	1.63	2.726	0.113	1.68	1.30	1.63
120x50x15 -1.2-200-17	28.12	3.675	29.22	1.64	2.842	0.105	1.68	1.31	1.66
150x60x15 -1.2-20-4	154.26	0.391	422.05	1.02	0.296	0.951	0.88	1.02	0.95
150x60x15 -1.2-30-5	147.42	0.587	389.65	1.03	0.444	0.874	0.92	1.01	1.01
150x60x15 -1.2-40-5	141.90	0.781	348.58	1.06	0.592	0.790	0.98	1.01	1.04
150x60x15 -1.2-50-5	138.63	0.975	302.33	1.13	0.738	0.701	1.08	1.04	1.08
150x60x15 -1.2-60-5	132.85	1.167	254.38	1.21	0.884	0.609	1.19	1.08	1.09
150x60x15 -1.2-70-6	125.95	1.359	207.77	1.32	1.029	0.523	1.31	1.14	1.06
150x60x15 -1.2-80-6	123.14	1.549	164.53	1.57	1.173	0.447	1.50	1.31	1.16
150x60x15 -1.2-90-7	118.44	1.737	130.79	1.84	1.316	0.382	1.69	1.46	1.14
150x60x15 -1.2-100-8	106.00	1.924	106.65	1.95	1.457	0.329	1.76	1.55	1.31
150x60x15 -1.2-110-8	85.36	2.108	88.79	1.83	1.597	0.285	1.63	1.46	1.31
150x60x15 -1.2-120-9	76.14	2.291	75.21	1.87	1.735	0.249	1.66	1.49	1.32
150x60x15 -1.2-130-5	67.15	2.471	64.64	1.87	1.871	0.220	1.66	1.49	1.38
150x60x15 -1.2-140-6	52.48	2.649	56.26	1.79	2.006	0.195	1.46	1.43	1.25
150x60x15 -1.2-150-6	44.06	2.824	49.49	1.72	2.139	0.175	1.37	1.37	1.21
150x60x15 -1.2-160-7	40.04	2.997	43.95	1.76	2.269	0.157	1.39	1.40	1.25
150x60x15 -1.2-170-8	36.64	3.166	39.36	1.68	2.398	0.143	1.40	1.34	1.29
150x60x15 -1.2-180-8	32.35	3.333	35.52	1.55	2.525	0.130	1.35	1.24	1.28
150x60x15 -1.2-190-9	27.94	3.498	32.26	1.39	2.649	0.119	1.27	1.11	1.23
150x60x15 -1.2-200-9	21.98	3.659	29.48	1.18	2.771	0.110	1.09	0.94	1.07
			Mean	1.38			1.42	1.16	1.25
			Std. Dev.	0.267			0.320	0.175	0.231
			Capacity reduction factor (φ)	0.85			0.85	0.85	0.85
			Reliability index (β)	3.28			3.04	2.97	2.87

7.2 Assessment of the Proposed design equations:

The applicability of the proposed equation has been verified by reliability analysis, comparing with test results and FEA results available in the literature (Vijayanand and Anbarasu 2019, Kherbouche *et al.* 2019). As shown in Table 3, the parametric study conducted by Kherbouche *et al.* (2019) was used in this study to compare its design strengths obtained with the design strengths of AISI and EC3 predicted by the proposed design equations.

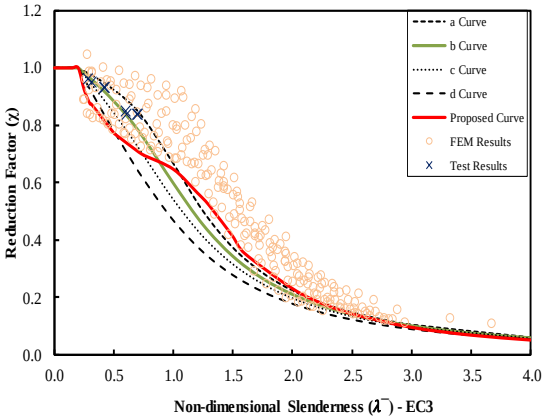

(a)

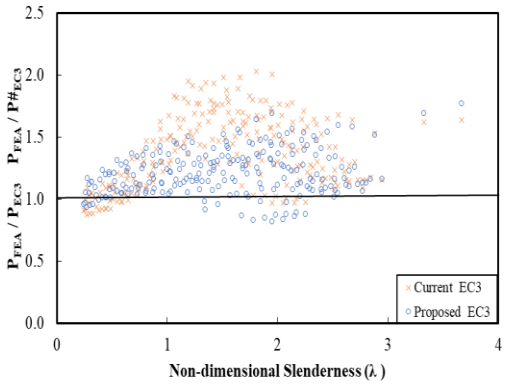

(b)

Fig. 5 Comparison of FEA results with EC3 and Proposed EC3

The mean and standard deviation of $P_{FEM}/P\#_{AISI}$ are 1.03 and 0.155 respectively. Similarly, the mean and standard deviation of $P_{FEM}/P\#_{EC3}$ are 1.13 and 0.291 respectively. It is observed that the equation proposed by Kherbouche *et al.* (2019) predicts the more conservative results when compared with the existing curve. Hence it is assessed that the proposed design equations will predict the reliability and consistency results for finding the accurate design strengths of the CFS built-up battened columns.

The test results available in the literature Vijayanand and Anbarasu (2016) are plotted in Figs. 4a and 5a to compare and current design rules of AISI and proposed AISI. It is observed that the Proposed AISI curve predicts better than the existing curve when comparing to test results also. Since the test results come under the low slenderness, the Proposed EC3 curve provides little conservative than the existing curve. Therefore it is proved that the proposed curves of both EC3 and AISI predict safe and reliable results.

7.3 Effect of slenderness Parameter

The effect of the slenderness parameter is assessed in Fig. 6. The ultimate compression capacity has been normalized by the product of gross area and the yield stress

Table 3 Verification of Proposed equation with FEM results of Kherbouche *et al.* (2019)

	FEA results available in the literature (Kherbouche *et al.* 2019)	
	$P_{FEM}/P\#_{AISI}$	$P_{FEM}/P\#_{EC3}$
Number of results	36	36
Mean	1.03	1.13
Standard Deviation	0.155	0.291

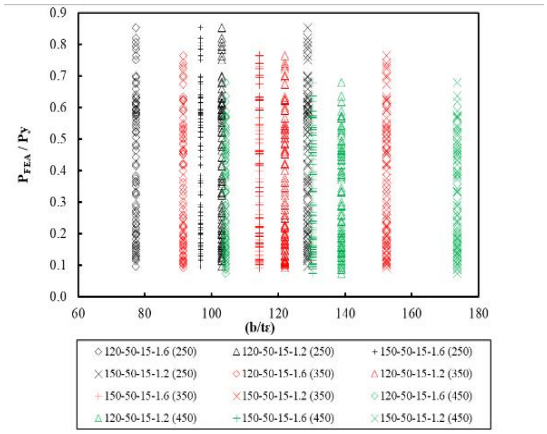

Fig. 6 Variation in P_{FEA}/P_y with (b/tƐ) ratios for AISI

(F_y) which is plotted against the slenderness parameter (b/tƐ) of the most slender constituent element in the cross-section controlling the local buckling response where 'Ɛ' is the material factor defined as $\varepsilon=\sqrt{(235/F_y)}$. In Fig. 6, it is observed that the ratio of P_{FEA}/P_y decreases for the higher slenderness parameter (b/tƐ). Also observed that the column series 120 x 50 x 50-1.2 having yield stress of 250 MPa with overall slenderness of around 90 were affected with a very little amount in terms of load-carrying capacity of the built-up columns.

7.4 Effect of Global column slenderness, Yield stress, and thickness

From Figs. 7 and 8, we can see the axial compressive strength dropped with an increase in the global column slenderness. Similarly, for all the column series, the axial compressive resistance reduced gradually with the change in the magnitude of yield stress from higher to lower.

It is also noticed that the axial strength has been increased while thickness of the built-up compression members is higher.

8. Conclusion

This paper presents a finite element investigation to predict the behaviour and ultimate axial load carrying capacity of the CFS built-up battened columns. While developing the finite element models, the Geometric nonlinearity, material nonlinearity, and initial geometric imperfections were considered. The finite element model was validated with the experimental results published in the companion paper. The comparison shows that there is good correlation between experimental results and finite element

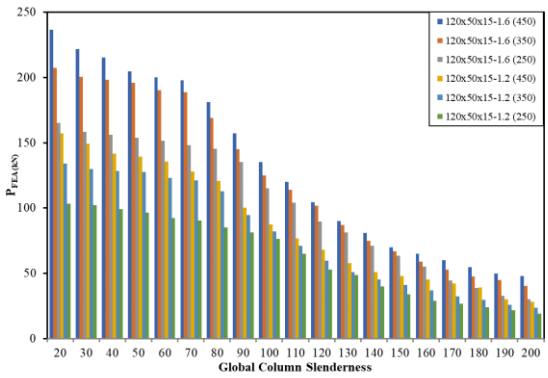

Fig. 7 FEA results Vs Global Column Slenderness for 120 x 50 x 15-1.6 and 1.2 series

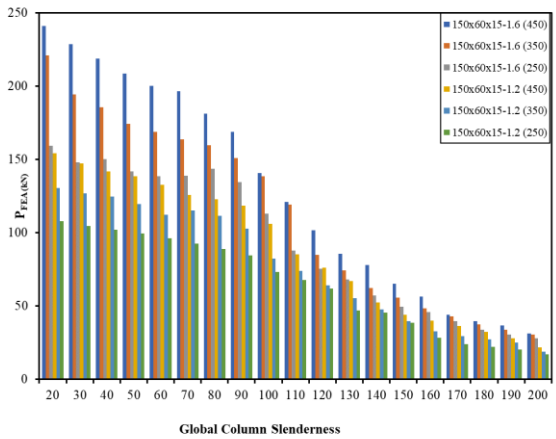

Fig. 8 FEA results Vs Global Column Slenderness for 150 x 60 x 15-1.6 and 1.2 series

results in terms of ultimate axial compressive load and deformed characteristic curves. The validated finite element model was used to conduct the parametric study to propose the design equation for the CFS built-up battened column. A total of 228 parametric analyses were conducted by influencing the parameters such as overall slenderness, plate slenderness, different geometry and yield stress of the built-up battened columns. The ultimate axial compressive loads obtained from the finite element analysis were compared with the design strengths determined from the design guidelines AISI (2016) and EC3. The following are the conclusions drawn from this study:

- The unbraced length of the column sections provided were within the maximum limit. Therefore, the provided unbraced length has been followed for the proposed curve for AISI and EC3
- It is found that the ratio of non-dimensional load (P_{FEA}/P_y) decreases with the increase of the slenderness parameter ($b/t\varepsilon$).
- The axial compressive strength of the CFS built-up battened columns is reduced when the global column slenderness increases.
- The axial compressive resistance reduced gradually with the changes in the magnitude of yield stress and thickness from higher to lower. Therefore it is concluded that the global column slenderness and plate slenderness affects the axial compressive load of the built-up battened columns.
- From the parametric study, it is also observed that both current design rules have the limitation in predicting the design strength of the CFS built-up battened columns accurately.
- The axial strengths calculated using the proposed design equations based on the effective width method of AISI and EC3 were less scattered, conservative and reliable. Hence it is recommended to adopt the proposed equations to determining the accurate ultimate resistance of the CFS Built-up battened columns.
- The reliability of the proposed design equations has been assessed with the FEA results available in the literature and also assessed with the test results of the author's companion paper. Hence it is concluded that the proposed design rules of AISI and EC3 give the safe and better results for the prediction of CFS Built-up battened columns.

References

ABAQUS (2014), ABAQUS Standard (Version 6.14.2), Simulia Inc., Johnston, RI, U.S.A.

AISI (2007), North American specification for the design of cold formed steel structural members, Washington, DC, U.S.A.

AISI (2016), North American specification for the design of cold formed steel structural members, Washington, DC, U.S.A.

Anbarasu, M. (2019a), "Simulation of flexural behaviour and design of CFS closed built-up beams composed of two sigma sections for local buckling", *Eng. Struct.*, **191**, 549-562. https://doi.org/10.1016/j.engstruct.2019.04.093.

Anbarasu, M., Kumar, S.B. and Sukumar, S. (2013), "Study on the effect of ties in the intermediate length cold formed steel (CFS) columns", *Struct. Eng. Mech.*, **46**(3), 323-335. https://doi.org/10.12989/sem.2013.46.3.323.

Anbarasu, M. and Sukumar, S. (2014), "Influence of spacers on ultimate strength of intermediate length thin walled columns", *Steel Compos. Struct.*, **16**(4), 437-454. https://doi.org/10.12989/scs.2014.16.4.437.

Anbarasu, M. and Venkatesan, M. (2019b), "Behaviour of CFS built-up I-section columns composed of four U-profiles", *Adv. Struct. Eng.*, **22**(3), 613-625. https://doi.org/10.1177/1369433218795568.

Anbarasu, M. and Dar, M. (2020), "Improved design procedure for battened cold-formed steel built-up columns composed of lipped angles", *J. Construct. Steel Res.*, **164**, 105781. https://doi.org/10.1016/j.jcsr.2019.105781.

AS1170.1-2002, Standards Association of Australia, Sydney, Australia.

ASCE (2006), Minimum design loads for buildings and other structures, ASCE/SEI7-05. American Society of Civil Engineers Standard; 2006., China, October.

Australian Standard, SAA Loading Code, Part1: Dead and Live Loads and Load Combinations.

Bandula Heva, Y. and Mahendran, M. (2012), "Flexural-torsional buckling tests of CFS compression members at elevated temperatures", *Steel Compos. Struct.*, **14**(3), 205-227. https://doi.org/10.12989/scs.2013.14.3.205.

Biggs, K.A., Ramseyer, C., Ree, S. and Kang, T.H.K. (2015), "Experimental testing of cold-formed built-up members in pure compression", *Steel Compos. Struct.*, **18**(6), 1331-1351.https://doi.org/10.12989/scs.2015.18.6.1331.

Dabaon, M., Ellobody, E. and Ramzy, K. (2015), "Experimental investigation of built-up CFS section battened columns", *Thin-Walled Structures*, **92**, 137-145. https://doi.org/10.1016/j.tws.2015.03.001.

Dar, M., Subramanian, N., Dar, A. and Raju, J. (2015a), "Experimental investigations on the structural behaviour of a distressed bridge", *Struct. Eng. Mech.*, **56**(4), 695-705. https://doi.org/10.12989/sem.2015.56.4.695.

Dar, M., Yusuf, M., Dar, A. and Raju, J. (2015b), "Experimental study on innovative sections for cold formed steel beams", *Steel Compos. Struct.*, **19**(6), 1599-1610. https://doi.org/10.12989/scs.2015.19.6.1599.

Dar, M. A., Subramanian N., Dar A. R., Anbarasu M., Lim J.B.P., (2018a), "Structural Performance of Cold-formed Steel Composite Beams", *Steel Compos. Struct.*, **27**(5), 545-554.

Dar, M.A., Sahoo, D.R., Pulikkal, S. and Jain, A.K. (2018b), "Behaviour of laced built-up CFS columns: Experimental investigation and numerical validation", *Thin Wall. Struct.*, **132**, 398-409. https://doi.org/10.1016/j.tws.2018.09.012.

Dar, M., Subramanian, N., Rather, A.I., Dar, A., Lim JBP, Anbarasu M. and Roy, K. (2019a), "Effect of angle stiffeners on the flexural strength and stiffness of cold-formed steel beams", *Steel Compos. Struct.*, **33**(2), 225-243.

Dar, M.A., Subramanian N., Dar A.R., Majid M., Haseeb M., Tahoor M., (2019b) "Structural efficiency of various strengthening schemes for cold-formed steel beams: Effect of global imperfections", *Steel Compos. Struct.,* **30**(4), 393-403.

Devi, S.V. and Singh, K.D. (2020), "Finite element study of lean duplex stainless steel semi-elliptical hollow section members with circular perforation subjected to torsion", *Thin Wall. Struct.*, **146** https://doi.org/10.1016/j.tws.2019.106464.

El Aghoury, M., Salem, A., Hanna, M. and Amoush, E. (2013), "Ultimate capacity of battened columns composed of four equal slender angles", *Thin Wall. Struct.*, **63**, 175-185.https://doi.org/10.1016/j.tws.2012.07.019.

El Aghoury, M., Salem, A., Hanna, M. and Amoush, E. (2015), "Strength of cold formed battened columns subjected to eccentric axial compressive force", *J. Construct. Steel Res.*, **113**, 58-70. https://doi.org/10.1016/j.jcsr.2015.04.008.

Eurocode 3 (2005), Design of steel structures-Part1-1: General rules and rules for building, BS EN 1993-1-1, London.

Eurocode 3 (2006), Design of steel structures-Part 1-3: General rules supplementary rules for cold-formed members and sheeting, BS EN 1993-1-3, Brussels.

Eurocode 3 (2006), Design of steels tructures-Part1-5: Plated structural elements, BS EN 1993-1-5, London.

Ghannam, M. (2017), "Axial load capacity of CFS built-up stub columns", *J. Steel Struct.*, **17**(4), 1273-1283. https://doi.org/10.1007/s13296-017-1202-0.

Gunalan, S. and Mahendran, M. (2013), "Improved design rules for fixed ended CFS columns subject to flexural–torsional buckling", *Thin Wall. Struct.*, **73**, 1-17. https://doi.org/10.1016/j.tws.2013.06.013.

Kherbouche, S. and Megnounif, A. (2019), "Numerical study and design of thin walled cold formed steel built-up open and closed section columns", *Eng. Struct.*, **179**, 670-682. https://doi.org/10.1016/j.engstruct.2018.10.069.

Kripka, M. and Chamberlain Pravia, Z.M. (2013), "CFS channel columns optimization with simulated annealing method", *Struct. Eng. Mech.*, **48**(3), 383-394. https://doi.org/10.12989/sem.2013.48.3.383.

Lu, Y., Li, W., Zhou, T. and Wu, H. (2017), "Novel local buckling formulae for cold-formed C-section columns considering end condition effect", *Thin Wall. Struct.*, **116**, 265-276. https://doi.org/10.1016/j.tws.2017.02.034.

Maia, W., Vieira Jr, L., Schafer, B. and Malite, M. (2016), "Experimental and numerical investigation of CFS double angle members under compression", *J. Construct. Steel Res.*, **121**, 398-412. https://doi.org/10.1016/j.jcsr.2016.03.003.

Megnounif, A., Djafour, M., Belarbi, A. and Kerdal, D. (2008), "Strength buckling predictions of CFS built-up columns", *Struct. Eng. Mech.*, **28**(4), 443-460. https://doi.org/10.12989/sem.2008.28.4.443.

Muftah, F., Sani, M., Hisyam, M.S., Muda, M.F. and Mohammad, S. (2014), "Assessment of Connection Arrangement of Built-up CFS Section under Axial Compression", *Adv. Mater. Res.*, https://doi.org/10.1002/cepa.224.

Muthuraj, H., Sekar, S., Mahendran, M. and Deepak, O. (2017), "Post buckling mechanics and strength of CFS columns exhibiting Local-Distortional interaction mode failure", *Struct. Eng. Mech.*, **64**(5), 621-640. https://doi.org/10.12989/sem.2017.64.5.621.

Roy, K., Ting, T.C.H., Lau, H.H. and Lim, J.B. (2018), "Nonlinear behavior of axially loaded back-to-back built-up CFS un-lipped channel sections", *Steel Compos. Struct.*, **28**(2), 233-250. https://doi.org/10.12989/scs.2018.28.2.233.

Sahoo, D.R. and Rai, D.C. (2007), "Built-up battened columns under lateral cyclic loading", *Thin-Walled Struct.*, **45**(5), 552-562. https://doi.org/10.1016/j.tws.2007.02.016.

Saleh, A., Zahrai, S.M. and Mirghaderi, S.R. (2016), "Experimental study on innovative tubular web RBS connections in steel MRFs with typical shallow beams", *Struct. Eng. Mech.*, **57**(5), 785-808. https://doi.org/10.12989/sem.2016.57.5.785.

Schafer, B.W., and Pecoz, T. (1998), "Computational modelling of cold-formed steel: characterizing geometric imperfections and residual stresses", *J. Construct. Steel Res.*, **47**(3), 193-210. https://doi.org/10.1016/S0143-974X(98)00007-8.

Serror, M.H., Soliman, E.G. and Hassan, A.F. (2017), "Numerical study on the rotation capacity of CFRP strengthened cold formed steel beams", *Steel Compos. Struct.*, **23**(4), 385-397. https://doi.org/10.12989/scs.2017.23.4.385.

Shi, G., Liu, Z., Ban, H., Zhang, Y., Shi, Y. and Wang, Y. (2012), "Tests and finite element analysis on the local buckling of 420 MPa steel equal angle columns under axial compression", *Steel Compos. Struct.*, **12**(1), 31-51. https://doi.org/10.12989/scs.2011.12.1.031.

Standards of Australia (2018), CFS Structures, AS/NZS 4600.

ValsaIpe, T., SharadaBai, H., ManjulaVani, K. and Iqbal, M.M.Z. (2013), "Flexural behavior of CFS concrete composite beams", *Steel Compos. Struct.*, **14**(2), 105-120. https://doi.org/10.12989/scs.2013.14.2.105.

Vijayanand, S. and Anbarasu, M. (2019), "Strength and behavior of cold-formed steel built-up battened columns: tests and numerical validation", *J. Struct. Eng. (Madras),* **46**(2), 154-164.

Whittle, J. and Ramseyer, C. (2009), "Buckling capacities of axially loaded, cold-formed, built-up C-channels", *Thin Wall. Struct.,***47**(2), 190-201. https://doi.org/10.1016/j.tws.2008.05.014.

Young, B. and Chen, J. (2008), "Design of CFS built-up closed sections with intermediate stiffeners", *J. Struct. Eng.*, **134**(5), 727-737. https://doi.org/10.1061/(ASCE)0733-9445(2008)134:5(727).

Zhang, J.H. and Young, B. (2015), "Numerical investigation and design of cold-formed steel built-up open section columns with longitudinal stiffeners", *Thin Wall. Struct.*, **89**, 178-191. https://doi.org/10.1016/j.tws.2014.12.011.

Zhang, J.H. and Young, B. (2018), "Finite element analysis and design of CFS built-up closed section columns with web stiffeners", *Thin-wall. Struct.*, **131**, 223-237. https://doi.org/10.1016/j.tws.2018.06.008.

Zhou, W. and Jiang, L. (2017), "Distortional buckling of cold-formed lipped channel columns subjected to axial compression", *Steel Compos. Struct.*, **23**(3), 331-338. https://doi.org/10.12989/scs.2017.23.3.331.

CC